

Simulation and Experiment of Ghost Imaging-OCT Target Imaging in Scattering Media

Decai Huyan^a, Nofel Lagrosas^b and Tatsuo Shiina^c

Graduate School of Science and Engineering, Chiba University, Chiba-shi, Japan

Keywords: OCT, Ghost Imaging, Scattering Media.

Abstract: Conventional optical coherence tomography (OCT) target imaging is easily affected by scattering media and gets error results in optical properties about transmittance and absorbance of the target. We propose a new system for this problem by combining the Ghost Imaging(GI) technique and OCT on the measurement path. Even if the modulated images by scatterers under its low signal-to-noise ratio, the GI technique can reconstruct the images in the situation. Our system uses a single detector in the 2D dimensions to get the target images in the scattering media by getting rid of the modulation. In this paper, we introduce the concept and demonstrate the experimental method of Ghost Imaging-OCT, we call GI-OCT. We get the same shape in the binarized images by comparing the GI-OCT experimental image with corrected modulation and the original image without modulation. In the simulation we obtained the PSNR value of 47dB at 10% noise rate. In the experiment we got the PSNR value of 18.89dB. The results prove our system is helpful for target imaging in the scattering media.


1 INTRODUCTION


Optical coherence tomography (OCT) is an imaging technique that can produce high-resolution tomographic images using a non-contact, non-invasive method on a non-homogeneous medium(Huang et al., 1991). Based on the principle of low coherence interference, OCT combines reflected light from the measurement and reference paths to recover the optical property distribution of an object at a depth direction. OCT systems have been used in commercial cases and have achieved great success in ophthalmology by providing detailed images from the inner retina. It has recently been used to diagnose cases in cardiology and dermatology(Gambichler et al., 2005). Moreover, OCT is also used in many biomedical multilayer scattering media, such as organs and skin(Spaide et al., 2018). This imaging technique is very important in early skin cancer detection and others.


This paper aims to detect no modulation target image in a scattering media. This modulation represents the scattering in the OCT image. No modulation means the OCT image is without the scattering.

In OCT measurements in scattering media, the target signal is always affected due to light attenuation and scattering in the scattering media as the measured light propagates in the depth direction. Such scattering attenuation of the OCT signal can be reduced by multi-angle incidence measurement and increasing the number of measurements. However, in unknown scattering media, these methods cannot eliminate the influence of the media on the target signal. The scattering media may change the direction of the measured light and cause a time delay. This makes it difficult to get an accurate shape of the target and to obtain an adequate image of the target in the scattering media.

Ghost imaging (GI) techniques have attracted attention because they distinguish between signal and noise. GI has been used in many fields since the publication of the paper "ghost imaging using a single detector"(Bromberg et al., 2009). In this paper, they presented that a single probe can illuminate a sample with different patterns of light multiple times, and reconstructed an image based on the relationship between the reflected light total intensity and the illuminated light pattern. We propose a new method to obtain target images in scattered media by combining Ghost Imaging and TimeDomain-OCT (GI-OCT)(Huyan et al., 2022). The proposed method

^a  <https://orcid.org/0000-0002-2490-0439>

^b  <https://orcid.org/0000-0002-8672-4717>

^c  <https://orcid.org/0000-0001-9292-4523>

in this paper can reconstruct images even when the signal-to-noise ratio is low due to scattering, using the ability of GI. By using this method, target images can be obtained without scattering effects.

2 DIFFERENT OF CONVENTIONAL OCT AND GI-OCT

Unlike conventional OCT, the OCT probe light from GI-OCT does not focus on a point but illuminates the light on an area, as in full field-OCT(FF-OCT). This method can take two-dimensional images with a single probe. FF-OCT enables imaging of target distribution because the camera directly takes a cross-sectional two-dimensional image perpendicular to the optical axis. However, FF-OCT cannot obtain target distribution without the effect of scattering. FF-OCT uses a megapixel camera to achieve cellular-level imaging. Each pixel in an FF-OCT image is a point measurement of the target, the same as conventional OCT(Vabre et al., 2002).

For ease of understanding, we show the target (scattered sample) in the scattering media in two parts on the OCT measurement. The former is the scatter layer before the light hits the target, and the latter is the target layer. When measuring the target layer in the scatter media with conventional OCT, a three-dimensional image can be constructed by changing the reference light path (A scan) and orthogonal motion of the probe (B scan) as shown in Figure 1(a). However, the reflected signal does always have scattering from the scatter layer, so the target layer distribution had modulated by scattering. For example, when measuring the optical properties (transmittance and absorbance) of a target layer with OCT, the distribution of the front scatter layer may change the direction of the light or delay the received signal of the target layer due to scattering. As a result, the modulated image of the optical properties of the target layer is detected.

Figure 1(b) illustrates the concept of GI-OCT, in which GI-OCT probe light passes through an expander and spatial light modulator (SLM), and the generated light patterns illuminate the target layer behind the scatter layer. Reflected light from the target and scatter layers are focused on a point detector. The A-scan signal of GI-OCT is a series of light intensities separated in the depth direction for each light illuminated pattern. Every A-scan signal can be separated as the sum of the illuminate pattern intensities for each layer distribution with the axial resolu-

tion of OCT. After repeated measurements with different light patterns, the correlation between those illuminated patterns and the sum of interference intensities of each separated layer is calculated by using the GI method to obtain each layer distribution. Each separated layer is reconstructed in a multilayer sample(3D).

Compared to conventional OCT measurements, GI-OCT acquires a two-dimensional image in the plane perpendicular to the optical axis with a single detector. Light misalignment to other directions and time delay in scattering media can be simultaneously summed and detected as OCT interference signals. The misalignment and delay are constructed as a scatter layer distribution. The target layer distribution and the former scattering layer distribution can be reconstructed using the same procedure. By the scatter layer distribution, the optical properties of the target layer can be corrected, and the target distribution is obtained without the scatter layer effects.

3 EXPERIMENT

Figure 3(a) shows the GI-OCT experiment setup. The GI-OCT uses the superluminescent diodes (SLD) light source with a central wavelength of 860 nm, Gaussian distribution, and an axial resolution of $10.1\mu\text{m}$. The reference path consists of a steady rotating motor and a fixed mirror to complete the axial scanning (A-scan)(Shiina et al., 2003). The measurement path of GI-OCT has the optical probe, which is composed of a collimator and two lenses to make the beam diameter expand. The DMD chip (DLP2000 DMD) is placed in the measurement area. The sample is set between the DMD chip and the optical probe.

There is a matrix corresponding to 640×360 and a total size of $4.84 \times 2.72\text{mm}$ micromirrors arranged inside the DMD chip. Each mirror size is $7.56 \times 7.56\mu\text{m}$, and the deflection angle is ± 12 degrees on the diagonal axis, divided into "on" and "off" states. Then, the DMD chip in our experiments is oriented towards the vertical optical axis 12 degree to obtain the reflected light from the DMD. DMD chips are rotated 45 degrees counterclockwise in the vertical plane against the optical axis to make the diagonal axis vertical too. Moreover, the DMD is tilted 12 degree against the optical axis when the micromirrors state is "on". Because of these tilts, this DMD orientation causes a series of interference signals in the time domain, as shown in Fig 3(b). In GI-OCT experiment, the DMD chip displays 10×10 speckles patterns in the area, which is $2 \times 2\text{mm}$ in size.

We prepare a sample with the target in the scatter-

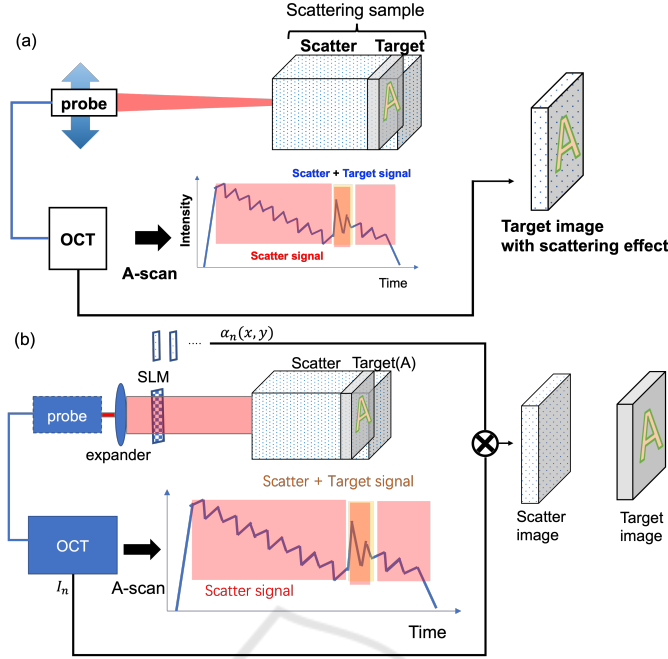


Figure 1: Setup of (a) a conventional OCT, that produces the target image with scattering influence. (b) GI-OCT, that produces the scatter image that can be used to generate the target image without the scattering influence. The difference between (a) and (b) is the presence of the beam expander and SLM in the GI-OCT setup.

ing media, and it has two layers: the first layer is the scatter layer, and the second layer is the target layer. Both layers are painted with water-based pigments on a slide glass. The target layer has the character "F", and the scatter layer was half-covered on the diagonal axis with paint. The water-based pigment adhered to the slide glass uniformly, and the pigment attenuation rate was 53%.

In our experiments, we set the DMD chip in the GI-OCT measurement area, and the reflected light from the DMD chip passes through the sample and returns to the probe. With this setup, the concept of GI-OCT about eliminating modulation becomes clear. Because the DMD chip is located in the measurement area, its reflection efficiency is high, resulting in more stable light intensity. This setup eliminates the influence from many different layers and focuses on reconstructing the target layer with one scattering layer.

However, we used four separate experiments for this experimental design to achieve our purpose. Experiment 1: OCT beam distribution measurement (not any layers); Experiment 2: target layer measurement; Experiment 3: scatter layer measurement; Experiment 4: target layer overlapping scatter layer measurement.

4 SIMULATION

To validate our proposed GI-OCT technique, we performed simulation experiments on the reconstruction of target imaging. First, we explain the evaluation method for the quality of the reconstructed image, which is the peak signal-to-noise ratio (PSNR) used for comparing the reconstructed of original image. It approximates human perception of reconstruction image quality and is calculated using Eq.(1).

$$PSNR = 10 \cdot \log_{10} \left(\frac{MAX^2}{MSE} \right) \quad (1)$$

MSE is the mean squared error of the original and reconstructed picture. MAX is the maximum possible pixel value in the image. In an 8-bit image, acceptance values for the PSNR in the original and reconstructed pictures should be over 30 dB to achieve a higher reconstruction quality.

In the OCT measurements, the quality of the OCT image is degraded by noise, due to the slight movement of the sample, limited light bandwidth, phase aberrations of propagating beam, the aperture of the detector, and multiple scattering within the coherence length. So we evaluate noise influence on the reconstructed image.

We implemented multiple GI methods, including computational ghost imaging (CGI), differential

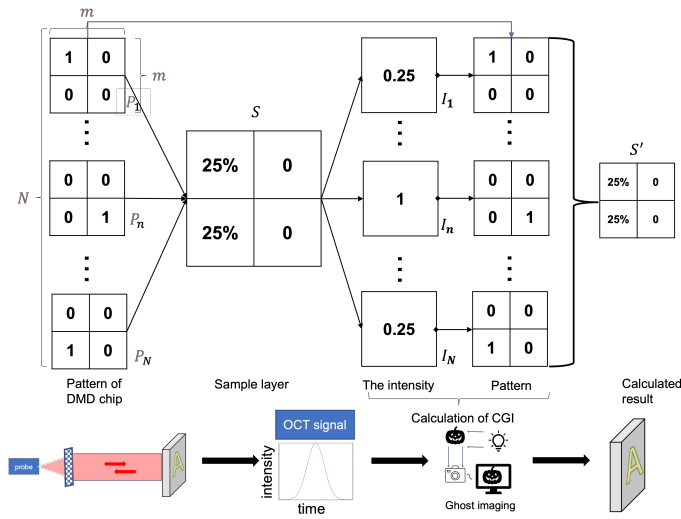


Figure 2: The steps of GI-OCT measurement: light pattern from the probe and SLM illuminates the sample to obtain the intensity of the OCT signal (intensity vs time graph) which can be calculated together with the pattern to produce the GI-OCT result. The matrices show the visualization of calculation process.

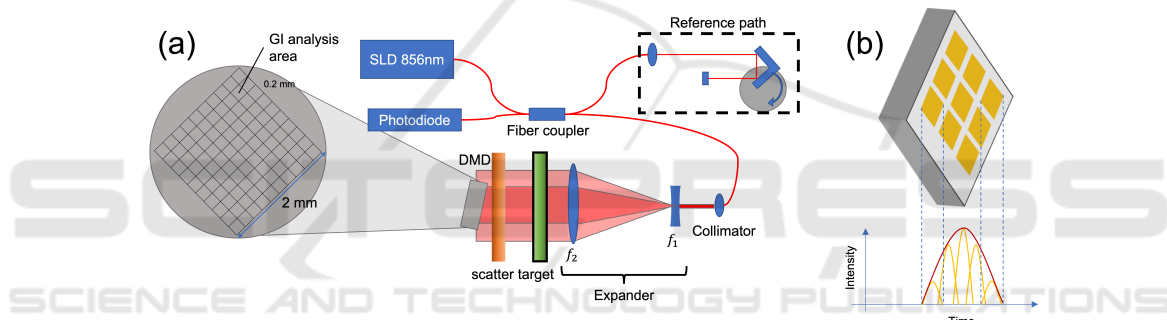


Figure 3: (a) Experiment set-up of GI-OCT. (b) The DMD micromirrors reflected signals in the time domain.

ghost imaging (DGI), pseudo-inverse ghost imaging (PGI), and differential pseudo-inverse ghost imaging (DPGI), to determine which one was appropriate for GI-OCT. (Ferri et al., 2010; Zhang et al., 2014) CGI is the calculation of pattern and light intensity, DGI is the difference between pattern and light intensity, PGI is the inverse matrix calculation of pattern and light intensity, and DPGI is the inverse matrix difference between pattern and light intensity. Between 90 and 1500 OCT measurements, we set noise at 10% of signal intensity in the OCT simulation (signal to noise ratio $\approx 10\%$). The simulation results with noise effects of reconstruction image quality are shown in Figure 4. The noise is the random value on each pattern in the gradation $-25 \sim 25$, which is 10% image value in the 8 bits image.

In Figure 4, starting with the number of measurements from 200 to 1500, the DPGI results are the best, and the PSNR value is beyond the acceptance value of 30 dB at the 800 measurements. PSNR's values of PGI, DGI and CGI are all below 30dB. It can be

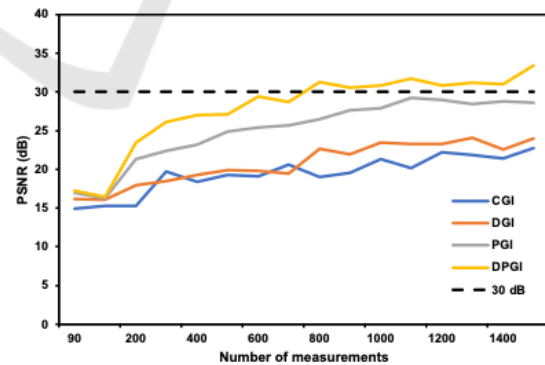


Figure 4: PSNR values derived from GI simulation with 10% noise.

concluded that the DPGI has the best reconstruction efficiency for our OCT application.

As shown in Figure 5, we simulated the scatter and target layers in the experiment. Based on the experiment, we used a 10×10 pixel resolution in this simulation. Figure 5 (a) shows the simulated scatter layer.

To simplify the calculation and to easily distinguish the effect of the scatter layer, we masked 1/4 of the area as a scatter layer. Figure 5 (b) shows the target layer obtained from the photograph of the letter 'T'. By loading a photograph with the letter 'T' and resizing it to 10×10 pixel image. Because the OCT beam is expanded in the GI-OCT measurement, causing the light intensity distribution affects the target result, we added the OCT beam to the simulation experiment, as shown in Figure 5 (c). By using the DPGI method on the 800 measurements with 10% random noise, the image from the GI-OCT measurement is obtained and shown in Figure 5 (d). Figure 5 (d) shows the image of target layer overlapping the scatter layer and OCT beam distribution with 10% random noise.

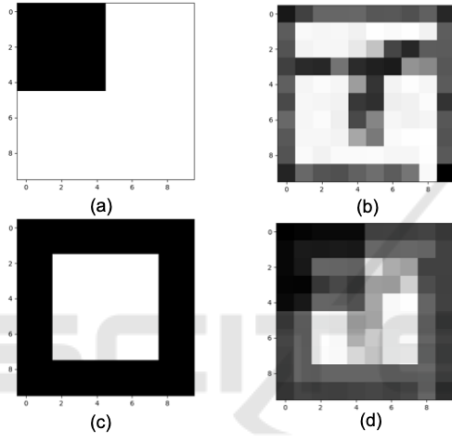


Figure 5: Simulation images. (a)scatter image. (b)light distribution. (c)target image. (d)overlaps (a), (b) and (c).

After correcting layer by layer with Figure 5 (d), we obtain the results of GI-OCT, as shown in Figure 6. Figure 6 (a) shows the simulation results after correcting the OCT beam distribution. This result is corrected in Figure 5 (d) using the OCT beam distribution in Figure 5 (c). Figure 6 (b) shows the result of the corrected target layer, which can be successfully identified as the letter 'T'. By calculating the PSNR value for the reconstructed image in Figure 6 (b) with the original image in Figure 5 (b), we get 47dB, which is acceptable. Not only that, but we also reconstructed the scatter layers and obtained Figure 6 (c). The reconstructed scatter layers have the same distribution as the original scatter layers in Figure 5 (c). Meanwhile, the OCT beam distribution(Figure 6c) is also reconstructed with the same result of Figure 5 (c).

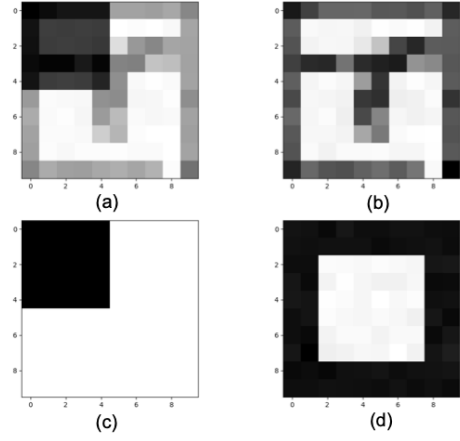


Figure 6: Simulation results. (a)target and scatter image corrected light distribution. (b)target image corrected scatter effect. (c)scatter image. (d)light distribution.

5 RESULTS

The distribution of the OCT beam, target layer, scatter layer, and the target layer overlapping the scatter layer was obtained from Experiments 1, 2, 3, and 4, respectively.

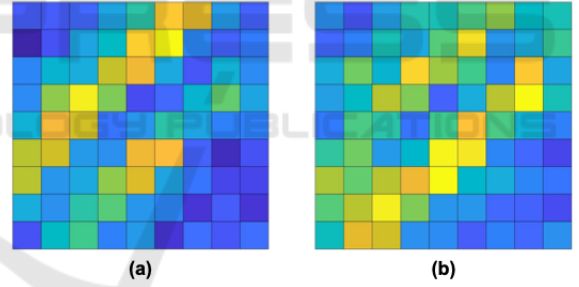


Figure 7: The results of GI-OCT. (a) target layer distribution overlapped beam distribution. (b) target layer distribution overlapped beam distribution and scatter layer distribution.

Figure 7 (a) is the target layer distribution. It is the result overlapped with the OCT probe beam distribution. A diagonal stroke can be seen from right upper to left bottom, similar to the vertical stroke of the character 'F'. It is difficult to identify the two horizontal strokes of the character 'F'. Figure 7 (b) is target layer overlapped by the scatter layer. This result have the OCT probe beam and the scatter layer distributions, too. No stroke of the character 'F' can be recognized.

We normalize each image of GI-OCT results from four experiments. First, we remove the OCT beam distribution from the target layer distribution to obtain Figure 8 (a). One stroke on the diagonal and two vertical strokes can be clearly identified, forming the

character "F". We also remove the scatter distribution from the target layer overlapped by the scatter layer distribution to obtain Figure 8 (b). And this process has recovered the OCT beam distribution.

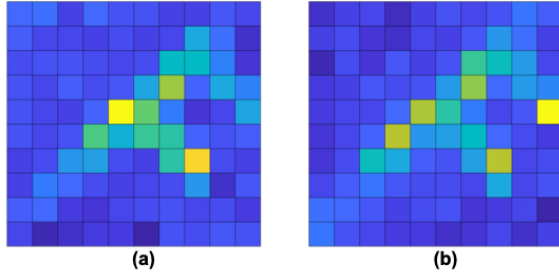


Figure 8: GI-OCT reconstructed images. (a) target layer distribution without beam distribution. (b) corrected target layer distribution without beam distribution and scatter layer distribution.

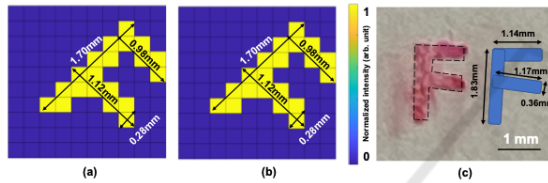


Figure 9: GI-OCT-reconstructed images with binarization of (a) original target layer image, (b) corrected target layer image.

Figure 8 (b) shows the same distribution of the character "F" as show in Figure 8 (a). We regard Figure 8 (a) as the original distribution of the target layer image, and Figure 8 (b) as the target layer image obtained after correction by scattering effects. The PSNR of the corrected target layer image in Figure 8 (b) is calculated to be 18.08 dB with the original target layer image in Figure 8 (a).

With an appropriate threshold value, binarization can result in Figures 9 (a) and (b) from Figures 8 (a) and (b). They have an identical distribution, and their PSNR is 160 dB. Moreover, we quantify the average stroke lengths of the character "F" in Figure 9 (c) and estimate the error rate to evaluate our experimental results. The error rate is the ratio of the stroke length of the reconstructed image to the length of the original target stroke. In Figure 9 (c), the length of the upper horizontal is 1.14mm, the middle horizontal is 1.17mm, and the vertical stroke is 1.83mm, and the widths of these strokes are 0.36mm. As compared to Figure 9 (a) and (b), we get the average length of the upper horizontal, middle horizontal, and vertical strokes, and their stroke widths are 0.98mm, 1.12mm, 1.70mm and 0.28mm, and the error rates are 14.0%, 4.2%, 7.1% and 22.2%, respectively. Errors in stroke lengths and widths are smaller than

0.2 mm.

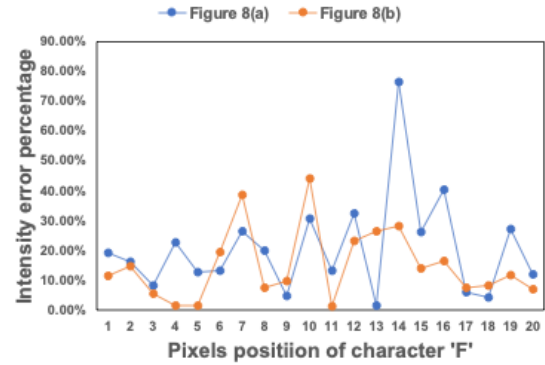


Figure 10: The intensity error percentages between (a) the original target layer compared with uniform distribution. (b) the corrected target layer compared with uniform distribution. The uniform distribution is the binarized ideal image in Fig.9.

As a result of the GI reconstruction, the target layer's total transmission can be adjusted to reorder the target's actual transmittance distribution. In our experiment, the original target layer's total transmission is 47%. And the total transmission of the corrected target layer is 47%, too. So we rearranged the transmission distribution in Figure 8 (a) and (b). The average transmission deviations in Figure 8 (a) and (b) are 20.0% and 14.8%, respectively. The deviation of each pixel is compared to an ideal uniform target layer distribution, as shown in Figure 9. The vertical coordinate is the deviation percentage of each pixel with the mean transmission. The horizontal coordinate indicates the pixel of the character from top to bottom in Figure 8 (a) and (b). This indicates that the solidification of the pigment is not uniform. Due to the limitation of the number of measurements and not 100% reproducibility of the pattern intensity, the target distribution is not completely consistent, so the transmission deviation trends are partly consistent in Figure 10. This deviation trend can be interpreted as the actual target transmittance distribution.

6 CONCLUSION

Our research aims to eliminate the scattering influence of scattering media on the target layer's optical properties, for which we propose a new method called GI-OCT. We simulated the measurement of a target layer affected by a scatter layer and added the effect of the OCT beam and noise during the measurement. The GI-OCT measurement method was used to obtain a target layer without the scattering effects. A PSNR value of 47 dB was obtained for the original

and corrected image by correcting the effects of the OCT beam and noise.

In the experiment, we successfully reconstruct the target layer distribution without scattering influence by using the GI technique to the OCT measurement path in a two-dimensional area. In the lower number of measurements, the PSNR value of our results is 18.08dB, but the target layer of character "F" can be identifiable. In the binarized images, we successfully acquired the target shapes without scattering effects and obtained the PSNR value of 160dB. The quantitative target length obtained an error smaller than the resolution, which is 0.2mm.

Our next step is to work on the scattering effects on image reconstruction in flowing scatter.

REFERENCES

- Bromberg, Y., Katz, O., and Silberberg, Y. (2009). Ghost imaging with a single detector. *Physical Review A - Atomic, Molecular, and Optical Physics*, 79(5):1–4.
- Ferri, F., Magatti, D., Lugiato, L. A., and Gatti, A. (2010). Differential ghost imaging. *Physical Review Letters*, 104(25):1–4.
- Gambichler, T., Moussa, G., Sand, M., Sand, D., Altmeyer, P., and Hoffmann, K. (2005). Applications of optical coherence tomography in dermatology. *Journal of Dermatological Science*, 40(2):85–94.
- Huang, D., Swanson, E. A., Lin, C. P., Schuman, J. S., Stinson, W. G., Chang, W., Hee, M. R., Flotte, T., Gregory, K., Puliafito, C. A., and Fujimoto, J. G. (1991). Optical coherence tomography. *Science*, 254(5035):1178–1181.
- Huyan, D., Lagrosas, N., and Shiina, T. (2022). Target imaging in scattering media using ghost imaging optical coherence tomography. *APL Photonics*, 7(8).
- Shiina, T., Moritani, Y., Ito, M., and Okamura, Y. (2003). Long-optical-path scanning mechanism for optical coherence tomography. *Applied Optics*, 42(19):3795.
- Spaide, R. F., Fujimoto, J. G., Waheed, N. K., Sadda, S. R., and Staurengi, G. (2018). Optical coherence tomography angiography. *Progress in Retinal and Eye Research*, 64(June 2017):1–55.
- Vabre, L., Dubois, A., and Boccara, A. C. (2002). Thermal-light full-field optical coherence tomography. *Opt. Lett.*, 27(7):530–532.
- Zhang, C., Guo, S., Cao, J., Guan, J., and Gao, F. (2014). Object reconstitution using pseudo-inverse for ghost imaging. *Optics Express*, 22(24):30063.